**Bone Regeneration with a Collagen Model Polypeptides/Alpha-Tricalcium Phosphate Sponge in a Canine Tibia Defect Model**

**Author names**
**Tomohiko Ito[1], Yoshiya Hashimoto[2], Shunsuke Baba[3], Tomio Iseki[4], Shosuke Morita[4]**

**Affiliations**
[1]Graduate School of Dentistry (First Department of Oral and Maxillofacial Surgery), [2]Department of Biomaterials, [3]Department of Oral Implantology, [4]First Department of Oral and Maxillofacial Surgery, Osaka Dental University, 8-1 Kuzuhahanazono-cho Hirakata, Osaka 573-1121, Japan

**Running title:** Bone Regeneration with a Collagen Model Polypeptides/Alpha-Tricalcium Phosphate Sponge

Abstract
***Introduction:*** We evaluated the effects of synthesized collagen model polypeptides consisting of a proline-hydroxyproline-glycine (poly(PHG)) sequence combined with porous alpha-tricalcium phosphate (α-TCP) particles on bone formation in a canine tibia defect model. ***Materials and Methods:*** The porous α-TCP particles were mixed with a poly(PHG) solution, and the obtained sponge was then cross-linked and characterized by X-ray diffraction and scanning electron microscopy (SEM). Tibia defects were analyzed in 12 healthy beagles using micro-computed tomography and histological evaluation. ***Results:*** At 2 and 4 weeks, the volume density of new bone was higher in the poly(PHG)/α-TCP group than poly(PHG) alone group ($p < 0.05$); however, there was no difference at 8 weeks ($p > 0.05$). Histological evaluation at 4 weeks after implantation revealed that the poly(PHG) had degraded and newly formed bone was present on the surface of the α-TCP particles. At 8 weeks, continuous cortical bone formation with a Haversian structure covered the top of the bone defects in both groups. ***Conclusion:*** This study demonstrates that the composite created using porous α-TCP particles and poly(PHG) is sufficiently adaptable for treating bone defects.
***Key Words: bone Regeneration, synthesized collagen model polypeptides, porous alpha-tricalcium phosphate***

## *Introduction*

In oral and maxillofacial surgery, bone defects commonly occur due to infections, trauma, tumors, and cysts, as well as clefts of the alveolar bone and palate. Bone resorption caused by periodontal diseases often results in tooth loss.[1] Autologous bone is widely regarded as the gold standard graft material.[2, 3] However, a limited amount of autologous bone can be harvested from an individual, and the procedure is relatively invasive. Therefore, scaffold materials are required, which should be bioabsorbable and able to be ultimately replaced by autologous tissue.[4] Furthermore, they should have superior handling characteristics for surgical applications, because conventional granular materials tend to leak from pores and are difficult to apply to bone defects.[5, 6]

The most popular scaffold materials are hydroxyapatite (HA), tricalcium phosphate (TCP), and tetracalcium phosphate, which are widely used in orthopedic and maxillofacial surgery because they show high biocompatibility and osteocompatibility.[7] Among the various calcium phosphate materials possible, previous studies have highlighted the potential of α-TCP particles as bone rebuilding materials, because they gradually biodegrade while bone regenerates around them.[8] For example, Kitamura et al.[9] developed an α-TCP porous body with a continuous pore structure via a relatively simple processing method involving a conventional sintering procedure—they used a slurry of β-TCP and potato starch to produce α-TCP that was in a thermodynamically stable phase at temperatures above 1,100°C.

Collagen has been widely applied clinically in various forms, such as gels or sponges, because it shows good biodegradability, biocompatibility, and absorbability.[1, 10] For example, collagen sponges are considered as a useful scaffold matrix for several types of tissues. Tanihara et al.[11] previously reported the chemical synthesis of collagen model polypeptides consisting of a proline-hydroxyproline-glycine (poly(PHG)) sequence that forms a triple-helical structure. Our previous study evaluated the effects of combining poly(PHG) and α-TCP particles on bone formation in a skull defect mini-pig model.[6] The material obtained by combining poly(PHG) and α-TCP particles did not induce inflammation and complete degradation and remodeling of the lamellar bone was observed.[6] However, the solution and particles combination was difficult to apply to bone defects, and showed a tendency to leak from defects.

Several novel peptide-based biomaterial scaffolds for tissue engineering have been reported[12]; however, it is still a great challenge to fabricate scaffolds for use in bone tissue engineering. In this study, we used a dehydrothermal cross-linking method to construct a poly(PHG) and porous α-TCP sponge as a scaffold for the bone regeneration. The effects of the poly(PHG)/α-TCP scaffold on bone regeneration were evaluated in surgically induced canine tibia defects.

## *Materials and Methods*

### *Synthesis of Poly(PHG)*

Poly(PHG) was synthesized according to previously published methods.[11] Briefly, PHG was dissolved in 10 mM phosphate buffer (pH 7.4) at a concentration of 165 mM, and mixed with 1-hydroxybenzotriazole (33 mM; Peptide Institute, Osaka, Japan) and 1-ethyl-3-(3-dimethyl-aminopropyl)-carbodiimide hydrochloride (825 mM; Peptide Institute). After sequential stirring for 2 hours at 4°C and 46 hours at 20°C, the reaction mixture was dialyzed against water for 48 hours to remove any residual reagents.

### *Preparation of Poly(PHG)/α-TCP Sponges*

The particles were prepared by pulverization of an α-TCP block with 80% of pores showing a continuous pore structures. Large and small α-TCP particles were provided by Taihei Chemical Industrial Co. Ltd. (Osaka, Japan). The median sizes of the large and small particles were 580.8 μm and 136.2 μm, respectively. The large and small α-TCP particles were mixed at mass ratios of 50:50 mass%. Next, α-TCP particles were mixed with the aqueous poly(PHG) solution at a concentration of 10mg/mL. In our previous study[1], the initial Young's modulus of β-TCP/atelocollagen sponge (0.2 g/mL) differed significantly from those of the other three composites (0.1, 0.05, and 0.02 g/mL). In this study, a composite sponge was not molded because there were too many granules at a 0.2 g/mL

mixing concentration of α-TCP and the poly(PHG) solution. Thus, the optimal mixing concentration of α-TCP and the poly(PHG) solution was determined to be 0.15 g/mL to produce the molded sponge. The mixture was then poured into plastic molds, and all samples were immediately frozen to −80°C and freeze-dried for 24 hours. The freeze-dried poly(PHG)/α-TCP constructs resembled sponge-like structures, and were subsequently cross-linked in vacuo at 140°C for 10 hours. The poly(PHG)/α-TCP sponges were sterilized with ethylene oxide gas at 40°C. The poly(PHG) sponges without α-TCP particles as a control were also prepared by same method.

X-ray diffraction (XRD) measurements of α-TCP
XRD measurements were performed using a Geigerflex diffractometer (Ultima IV; Rigaku, Tokyo, Japan) with Cu Ka radiation generated at 40 kV and 40 mA. The scan rate was 48/min with a step size of 0.028 over a 2u range of 10–80°.

*Establishment of the Animal Model*
Twelve healthy beagles 2 years of age and weighing approximately 10 kg were obtained from Hamaguchi Animal (Osaka, Japan) and used as the tibia defect model. The canines were housed in a temperature controlled environment at 24°C and were allowed food and water ad libitum. The body weight and general health of the canines were monitored throughout the study.

*Transplantation Procedures*
All procedures in this work were approved by the Animal Experiment Committee of Osaka Dental University and conformed to procedures described in the Guiding Principles for the Use of Laboratory Animals (approval number12-12001, 13-03026).

An initial incision was made in the skin covering an appropriate part of the tibia, and the skin and subcutaneous tissue were separated from the periosteum. A second incision was made in the periosteum of the tibia, and the periosteum was elevated and carefully dissected from the underlying tibia and identical defects (4 mm diameter, 6 mm depth) were made using a twist drill (Astra Tech, Tokyo, Japan) with physiologic saline cooling under general anesthesia (0.5 mg/kg pentobarbital sodium) and infiltration anesthesia (1.8 ml 2% lidocaine hydrochloride and 1:80,000 epinephrine). The defects were randomly filled with one of the two treatments as follows: the experimental group (animals with a transplanted mixture of poly(PHG) and α-TCP) and the control group (animals transplanted with poly(PHG) alone). Assessments were made at three different time periods (2, 4, and 8 weeks) after surgery. The periosteum and skin over the defects were then sutured in two layers (3-0 Vicryl; Ethicon GmbH & Co. KG, Norderstedt, Germany and 3-0 MANI SILK; MANI, INC, Tochigi, Japan). Six cavities were studied and tissues were histopathologically assessed at each follow-up time in each group.

*Radiographic Analysis*
The tibias were harvested for microradiographic examination using an SMX-130CT micro-computed tomography (CT) apparatus (Shimadzu, Kyoto, Japan). Blocks of bone specimens were mounted on the turntable. The exposure conditions were 51 kV and 120 mA. The data obtained from each slice were saved at 512 × 512 pixels. TRI/3D BON software (Ratoc Co. Ltd., Tokyo, Japan) was used to create a three-dimensional (3D) reconstruction image using the volume rendering method for morphological observations. In the 3D analysis, the total volume (TV; $cm^3$) and bone volume (BV; $cm^3$) were measured using the TRI/3D-BON software based on the obtained CT values. The volumetric density (VD) was then calculated based on the following formula: VD (%) = BV/TV.

*Histological Assessment*
The tibias were fixed in 10% neutral-buffered formalin (Sigma, St. Louis, MO, USA), demineralized in a solution of ethylenediaminetetraacetic acid (Sigma), dehydrated in a series of alcohol washes, and embedded in paraffin. The tibias were sectioned (5–7 μm) in the coronal plane and stained with hematoxylin and eosin (HE). Each section was observed using a BZ9000 All-in-One Fluorescence Microscope (Keyence, Tokyo, Japan). A fluorescence filter was used to visualize the remaining

poly(PHG) fragment and α-TCP particles.

*Statistical Analysis*

The mean and standard deviation of each parameter were calculated for each group and compared using the Student's *t*-test by using statistical software (Statcel2; OMS Publisher, Tokorozawa, Japan). A value of $p < 0.05$ was considered to be significant.

***Results***

*Porous α-TCP particles*.
Fig. 1 shows a scanning electron microscope (SEM) image of the synthesized porous ceramic particles. The ceramic body had a continuous pore structure, with a pore diameter of approximately 5–10 μm.

*Characteristics of the poly(PHG)/α-TCP sponge.*
Fig. 2 shows the general morphology of the poly(PHG)/α-TCP sponge. Fig. 3**A** shows the appearance of poly(PHG)/α-TCP, and Fig. 3**B** shows the microstructure of poly(PHG). The composites were composed of α-TCP particles and a 3D porous structure (with an anatomizing network).

*XRD Measurements of α-TCP Particles.*
Fig. 4 shows the XRD patterns of the poly(PHG)/α-TCP sponge and the α-TCP particles. The diffraction peaks of poly(PHG)/α-TCP (Fig. 4**A**) were reduced compared to those of the original α-TCP particles (Fig. 4**B**). However, a comparison of the scatter plot data of the synthesized α-TCP particles against α-TCP data registered with the Joint Committee on Powder Diffraction Standards (JCPDS) confirmed that these peaks appeared at the same angles.

*Microradiography*.
Representative 3D reconstructions of the filled defects in the poly(PHG)/α-TCP (experimental) and poly(PHG) alone (control) groups at 2, 4, and 8 weeks are presented in Fig. 5. In the experimental group, an impermeable image similar to that of the original α-TCP particles was observed at 2 weeks, and the amount of new bone increased over time so that the entire volume of each defect was filled with newly formed bone with a trabecular structure at 8 weeks. In the control group, the defects were empty and showed dense formation from the edge of the defect toward the center, with thickening observed between 4 and 8 weeks.

The VDs of each group at the three time points are shown in Fig. 6. At 2 and 4 weeks post-transplantation, the VDs in the experimental group were higher than those of the control group ($p < 0.05$). However, no significant difference in VD was observed between the two groups at 8 weeks post-transplantation ($p > 0.05$).

*Histological Assessment at 2 Weeks.*
The remaining poly(PHG) fragments and α-TCP particles appeared as fluorescent green and black, respectively, under the microscope (Fig. 7**C** , **F**). The poly(PHG)/α-TCP and poly(PHG) used to fill defects in the experimental and control groups, respectively, were not degraded (Fig. 7). In the experimental group, α-TCP particles were encapsulated by connective tissue, and the inflammatory reaction was minimal. High numbers of osteoblasts and new blood vessels were observed around α-TCP particles. Large, foreign cells resulting from the inflammatory response were observed, but were reduced in number compared to the control group (Fig. 7**B**, **E**).

*Histological Assessment at 4 Weeks.*
The remaining poly(PHG) fragments and α-TCP particles appeared as fluorescent green and black, respectively (Fig. 8**C**, **F**). In the experimental group (Fig. 8**A**, **B**, **C**), the α-TCP particles remained, and a reticulate structure was observed inside the particles. The newly formed, woven bone was directly deposited on the surface of the α-TCP particles and was also formed from the edge of the bone defect. Furthermore, the newly formed bone was interconnected and several osteocytes could be observed in an irregular pattern. By contrast, the poly(PHG) was remarkably degraded and was surrounded by connective tissue. In the control group (Fig. 8**D**, **E**, **F**), many poly(PHG) fragments also remained; however, some fragments of the implanted poly(PHG) were replaced by connective tissue similar to immature bone. The numbers of large foreign cells in both group were substantially decreased compared to those observed at 2 weeks post-surgery (Fig. 8).

*Histological Assessment at 8 Weeks.*

In both the experimental and control groups (Fig. 9), poly(PHG)/α-TCP particles were degraded and poly(PHG) was almost completely substituted by newly formed bone. A large number of osteoblasts were observed around newly formed bone, and bone formation appeared to have progressed in both groups (Fig. 9**B**, **E**). As a result, continuous cortical bone formation with Haversian structure covered the top of the bone defect and no histological marker indicative of an inflammatory response was observed in either group.

***Discussion***

Although autologous bone is considered to be the best grafting material, considerable effort has gone into the development of resorbable bone substitutes for use in the repair of periodontal osseous defects and alveolar ridge augmentation.[13, 14] In this study, we fabricated a biodegradable sponge composite for bone regeneration by combining porous α-TCP and poly(PHG). The poly(PHG)/α-TCP sponge can be easily cut with scissors or a sharp knife, and therefore, can be easily molded for use in alveolar bone augmentation. We evaluated the effects of this sponge on bone regeneration after implantation in canine tibia defects.

Calcium phosphate ceramics have been widely used to fill bone defects because of their osteoconductivity.[15] The in vivo degradation rate of TCP is higher than that of HA. In addition, α-TCP dissolves more easily in water than β-TCP even though they have exactly the same chemical composition.[16] Uchino et al.[17] found that HA formation is rarely observed on the surface of porous α-TCP ceramics with 80% porosity. In the present study, the composite sponge was fabricated by mixing poly(PHG) solution and porous α-TCP. However, the XRD pattern of poly(PHG)/α-TCP was not particularly different from that of α-TCP.

TCP's porous body gradually dissolves away from bone defects during bone repair, allowing for its substitution by regenerated bone.[18] Such a bioabsorbable ceramic with macropores is attractive for use as a bone filler in medical applications because its porous structure allows cell invasion.[18] However, the solubility of porous α-TCP might be higher than that of the original α-TCP, making it liable to be completely resorbed in the body before a bone defect can be repaired by bone regeneration. Kitamura et al.[9] reported that a higher degree of bone in-growth seemed to occur in porous α-TCP by coating it with an organic polymer. In vivo evaluation further showed that such a coating is effective for controlling the degradation rate of implanted α-TCP. In this study, we expected that the mixture of porous α-TCP and poly(PHG) would be similarly effective.

The particle size of bone graft materials is an important determinant of their osteogenic activity.[19, 20] The particle size also affects the quantity of the newly formed bone. The effects of combining poly(PHG) and α-TCP particles of various median sizes (large: 580.8 μm; small: 136.2 μm; or large and small mixed: 499.3 μm) on bone formation were evaluated in our previous study using a skull defect model in mini-pigs, and we showed that the bone formation and healing processes were faster in the mixed group than in the large or small groups.[6] This suggested that small α-TCP particles might initiate new bone formation and induce absorption of the large particles and replacement by mature bone.[6] In the present study, the large and small α-TCP particles mixed at mass ratios of 50:50 weight% were used in the fabrication of the sponge.

Collagen has been conventionally applied in clinical settings in various forms, such as gels or sponges, since it shows good biocompatibility and absorbability. Atelocollagen molecules do not contain telopeptides, and tend to show extremely low antigenicity when adopted as basic materials for medical use. [21] Our previous study demonstrated that composites created using α- or β-TCP particles and collagen sponges possessed adequate mechanical strength and were sufficiently adaptable for treating rat calvarias or canine tibia bone defects, respectively.[1, 5] However, the major disadvantages of using natural collagens of animal origin, such as atelocollagen, are the potential for antigenicity, pathogen pollution, and nonspecific cell adhesion.[22] By contrast, poly(PHG) removes the danger of pathogen pollution associated with animal-derived collagens and could self-assemble and form 2D and 3D structures.[11] Naturally, collagen fibers and other starting materials in implant materials tend to degrade soon after implantation. Tanihara[11] found that the rate of biodegradation of a poly(PHG) sponge implanted subcutaneously in a rat dorsal was nearly the same as that of Terudermis®, which is made from bovine type I atelocollagen.

Micro-CT has high resolution and only requires very thin tissue slices. With a larger number of slices the spatial differences within areas of the specimen become negligible.[23] In our study, micro-CT analysis showed that the VD in the experimental group was higher than that of the control at 2 and 4 weeks post-transplant, but not at 8 weeks. At 2 weeks, the high VD in the experimental group was not due to new bone formation but rather to the density of the remaining α-TCP. At 4 weeks, the density of the newly formed replacement bone was higher than that of the control group. However, at 8 weeks, the defects were almost completely filled with newly formed bone in both groups.

The processes of in vivo mineralization and biodegradation are complex for a composite scaffold. The balance of mineral deposition, biodegradation, and tissue regeneration changes greatly at different times after transplantation. In both the control and experimental groups, the absorption of poly(PHG) and α-TCP had started by 2 weeks and was completely finished by 8 weeks when it was replaced by a network of newly formed bone. In our previous study [1], the atelocollagen sponge-only scaffold was completely degraded at 4 weeks after implantation in a canine tibia model. Although the sponge scaffold was replaced not only by soft connective tissue but also by newly formed bone, the new bone did not show the formation of a typical bone network. The reason for this discrepancy might be related to differences of biodegradation between atelocollagen and poly(PHG) sponges. In the present study, some poly(PHG) remained at 4 weeks after implantation and was replaced by a network of newly formed bone. The physical characteristics of α-TCP result in higher and earlier remodeling activity than β-TCP [24], and the degradation rates of the porous α-TCP used in the present study are expected to be faster than the original α-TCP. The slow degradation rate of poly(PHG) combined with the rapid degradation of porous α-TCP balanced to match the rate of bone tissue regeneration. Thus, the poly(PHG)/α-TCP sponge we fabricated showed faster and better bone induction capacities compared to the poly(PHG) sponge. In addition, the remaining α-TCP particles in the defect were in direct contact with the newly formed bone. Osteogenic progenitor cells migrated from the adjacent bone edge or bottom, adhered to the surface of the α-TCP particles, and subsequently formed new bone. These results suggest that the adequate 3D porous structure consisting of poly(PHG) and α-TCP particles served to provide an appropriate spatial arrangement for the osteogenetic cells as well as to facilitate vascular invasion.

**Conclusion**

This study demonstrated that a sponge created using porous α-TCP particles and poly(PHG), which is a chemically synthesized collagen model polypeptide, is sufficiently adaptable for treating bone defects. Furthermore, the biodegradable poly(PHG)/α-TCP sponge was replaced by newly formed bone without any adverse responses. Therefore, this newly developed sponge composite may be useful for bone tissue engineering. The dehydrothermally cross-linked poly(PHG)/α-TCP sponge can be easily shaped, and therefore easily molded for applications to treat various tissue disorders such as periodontal bone defects, cyst cavities and alveolar bone augmentation.

Acknowledgments

We would like to thank Dr. Isumi Toda (Osaka Dental University, Osaka, Japan) for excellent technological support.

REFERENCES


1. Matsuno T, Nakamura T, Kuremoto K, Notazawa S, Nakahara T, Hashimoto Y, Satoh T, Shimizu Y. Development of beta-tricalcium phosphate/collagen sponge composite for bone regeneration. *Dent Mater J* 2006; **25**: 138-144.
2. Cohen M, Polley JW, Figueroa AA. Secondary (intermediate) alveolar bone grafting. *Clin Plast Surg* 1993; **20**: 691-705.
3. Baba S, Inoue T, Hashimoto Y, Kimura D, Ueda M, Sakai K, Matsumoto N, Hiwa C, Adachi T, Hojo M. Effectiveness of scaffolds with pre-seeded mesenchymal stem cells in bone regeneration - Assessment of osteogenic ability of scaffolds implanted under the periosteum of the cranial bone of rats. *Dent Mater J* 2010; **29**: 673-681.
4. Schliephake H, Kage T. Enhancement of bone regeneration using resorbable ceramics and a polymer-ceramic composite material. *J Biomed Mater Res* 2001; **56**: 128-136.
5. Arima Y, Uemura N, Hashimoto Y, Baba S, Matsumoto N. Evaluation of bone regeneration by porous alpha-tricalcium phosphate/atelocollagen sponge composite in rat calvarial defects. *Orthodontic Waves* 2013; **72**: 23-29.
6. Sakai K, Hashimoto Y, Baba S, Nishiura A, Matsumoto N. Effects on bone regeneration when collagen model polypeptides are combined with various sizes of alpha-tricalcium phosphate particles. *Dent Mater J* 2011; **30**: 913-922.
7. Kihara H, Shiota M, Yamashita Y, Kasugai S. Biodegradation process of α-TCP particles and new bone formation in a rabbit cranial defect model. *J Biomed Mater Res B* 2006; **79**: 284-291.
8. Wiltfang J, Merten HA, Schlegel KA, Schultze-Mosgau S, Kloss FR, Rupprecht S, Kessler P. Degradation characteristics of alpha and beta tri-calcium-phosphate (TCP) in minipigs. *J Biomed Mater Res* 2002; **63**: 115-121.
9. Kitamura M, Ohtsuki C, Iwasaki H, Ogata SI, Tanihara M, Miyazaki T. The controlled resorption of porous α-tricalcium phosphate using a hydroxypropylcellulose coating. *J Mater Sci Mater Med* 2004; **15**: 1153-1158.
10. Yamamoto Y, Nakamura T, Shimizu Y, Matsumoto K, Takimoto Y, Kiyotani T, Sekine T, Ueda H, Liu Y, Tamura N. Intrathoracic esophageal replacement in the dog with the use of an artificial esophagus composed of a collagen sponge with a double-layered silicone tube. *J Thorac Cardiovasc Surg* 1999; **118**: 276-286.
11. Tanihara M, Kajiwara K, Ida K, Suzuki Y, Kamitakahara M, Ogata S. The biodegradability of poly(Pro-Hyp-Gly) synthetic polypeptide and the promotion of a dermal wound epithelialization using a poly(Pro-Hyp-Gly) sponge. *J Biomed Mater Res A* 2008; **85**: 133-139.
12. Holmes TC. Novel peptide-based biomaterial scaffolds for tissue engineering. *Trends Biotechnol* 2002; **20**: 16-21.
13. Knabe C, Berger G, Gildenhaar R, Howlett CR, Markovic B, Zreiqat H. The functional expression of human bone-derived cells grown on rapidly resorbable calcium phosphate ceramics. *Biomaterials* 2004; **25**: 335-344.
14. Murugan R, Ramakrishna S. Bioresorbable composite bone paste using polysaccharide based nano hydroxyapatite. *Biomaterials* 2004; **25**: 3829-3835.
15. Kihara H, Shiota M, Yamashita Y, Kasugai S. Biodegradation process of alpha-TCP particles and new bone formation in a rabbit cranial defect model. *J Biomed Mater Res B Appl Biomater* 2006; **79**: 284-291.
16. Rojbani H, Nyan M, Ohya K, Kasugai S. Evaluation of the osteoconductivity of α-tricalcium phosphate, ß-tricalcium phosphate, and hydroxyapatite combined with or without simvastatin in rat calvarial defect. *Journal of Biomedical Materials Research - Part A* 2011; **98 A**: 488-498.
17. Uchino T, Ohtsuki C, Kamitakahara M, Tanihara M, Miyazaki T. Apatite formation behavior on tricalcium phosphate (TCP) porous body in a simulated body fluid. *Key Eng Mater* 2006; **309-311 I**: 251-254.
18. Kitamura M, Ohtsuki C, Ogata SI, Kamitakahara M, Tanihara M, Miyazaki T. Mesoporous calcium phosphate via post-treatment of α-TCP. *J Am Ceram Soc* 2005; **88**: 822-826.
19. Shapoff CA, Bowers GM, Levy B. The effect of particle size on the osteogenic activity of

composite graft of allogeneic freeze-dried bone and autogenous marrow. *J Periodontol* 1980; **51**: 625-630.
20. Zaner DJ, Yukna RA. Particle size of periodontal bone grafting materials. *J Periodontol* 1984; **55**: 406-409.
21. Itoh H, Aso Y, Furuse M, Noishiki Y, Miyata T. A honeycomb collagen carrier for cell culture as a tissue engineering scaffold. *Artif Organs* 2001; **25**: 213-217.
22. Aguzzi A, Montrasio F, Kaeser PS. Prions: health scare and biological challenge. *Nat Rev Mol Cell Biol* 2001; **2**: 118-126.
23. Tobita K, Ohnishi I, Matsumoto T, Ohashi S, Bessho M, Kaneko M, Matsuyama J, Nakamura K. Effect of low-intensity pulsed ultrasound stimulation on callus remodelling in a gap-healing model EVALUATION BY BONE MORPHOMETRY USING THREE-DIMENSIONAL QUANTITATIVE MICRO-CT. *J Bone Joint Surg* 2011; **93**: 525-530.
24. Wiltfang J, Merten HA, Schlegel KA, Schultze-Mosgau S, Kloss FR, Rupprecht S, Kessler P. Degradation characteristics of α and β tri-calcium-phosphate (TCP) in minipigs. *J Biomed Mater Res* 2002; **63**: 115-121.

Fig. 1. Photograph of poly(PHG)/α-TCP sponge. Scale = 20.0 mm.

Fig. 2. Scanning electron microscope image of porous α-TCP particles. Scale = 15.0 μm.

Fig. 3. Scanning electron microscope image of poly(PHG)/α-TCP **A** and poly(PHG) **B**. The asterisk respectively indicates poly(PHG) fragments and porous α-TCP particles. Scale = 200 μm.

Fig. 4. X-ray diffraction pattern of poly(PHG)/α-TCP **A** and porous α-TCP particles **B**.

Fig. 5. Micro-computed tomography images at 2, 4, and 8 weeks after surgery. The volumetric density (VD %) is calculated as bone volume (BV) /total volume (TV) (yellow box). Co: cortical bone side, Ma: marrow bone side.

Fig. 6. Volumetric densities (%) of each group reflecting the quantity of new bone at 2, 4, and 8 weeks after surgery.

Fig. 7. Light microscopic images of hematoxylin and eosin-stained sections of defects at 2 weeks. **A** Experimental group, lower magnification; **B** experimental group, higher magnification; **C** experimental group, higher magnification using a fluorescence filter; **D** control group, lower magnification; **E** control group, higher magnification; **F** control group, higher magnification using a fluorescence filter. Asterisk: poly(PHG); TCP: α-TCP particle; CT: connective tissue; NB: new bone; black arrow: capillary; black dot arrow: large foreign cells. Scale =**A**, **D** 10 mm. **B**, **C**, **E** and **F** = 100 μm.

Fig. 8. Light microscopic images of hematoxylin and eosin-stained sections of defects at 4 weeks. **A** Experimental group, lower magnification; **B** experimental group, higher magnification; **C** experimental group, higher magnification using a fluorescence filter; **D** control group, lower magnification; **E** control group, higher magnification; **F** control group, higher magnification using a fluorescence filter. Asterisk: poly(PHG); TCP: α-TCP particle; CT: connective tissue; NB: new bone; black arrow: capillary; black dot arrow: large foreign cells. Scale = **A**, **D** 10 mm. **B**, **C**, **E** and **F** = 100 μm.

Fig. 9. Light microscopic images of hematoxylin and eosin-stained sections of defects at 8 weeks. **A** Experimental group, lower magnification; **B** experimental group, higher magnification; **C** experimental group, higher magnification using a fluorescence filter; **D** control group, lower magnification; **E** control group, higher magnification; **F** control group, higher magnification using a fluorescence filter. Asterisk: poly(PHG); TCP: α-TCP particle; CT: connective tissue; NB: new bone; black arrow: capillary; black triangle: osteoblasts. Scale =**A**, **D** 10 mm. **B**, **C**, **E** and **F** = 100 μm.

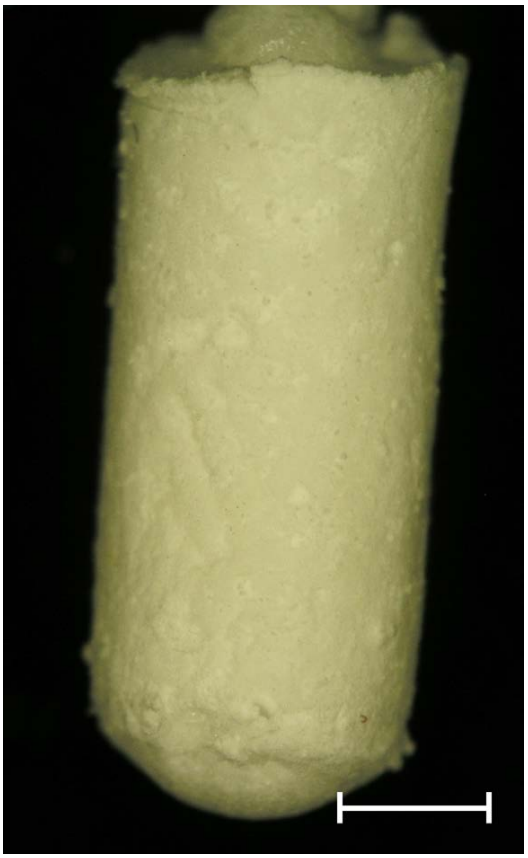

Fig. 1.

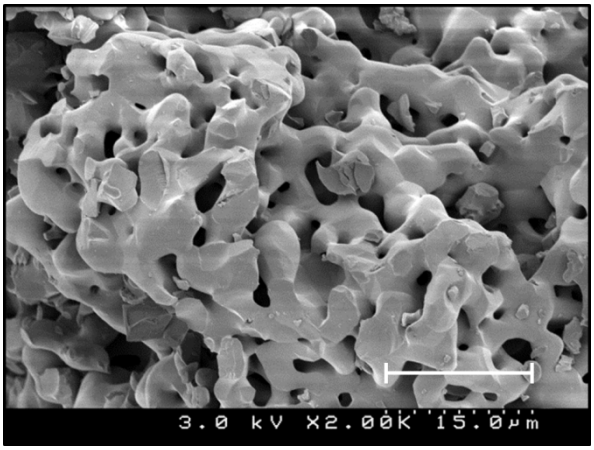


Fig. 2.

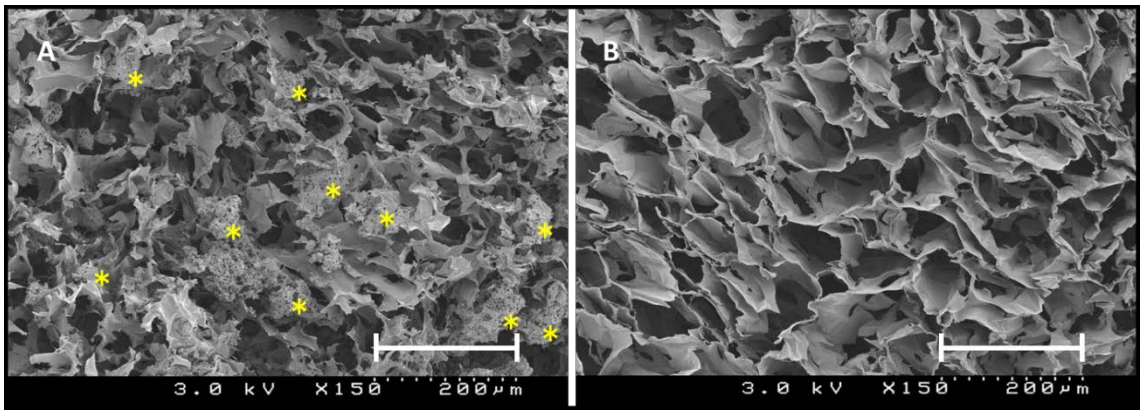


Fig. 3.

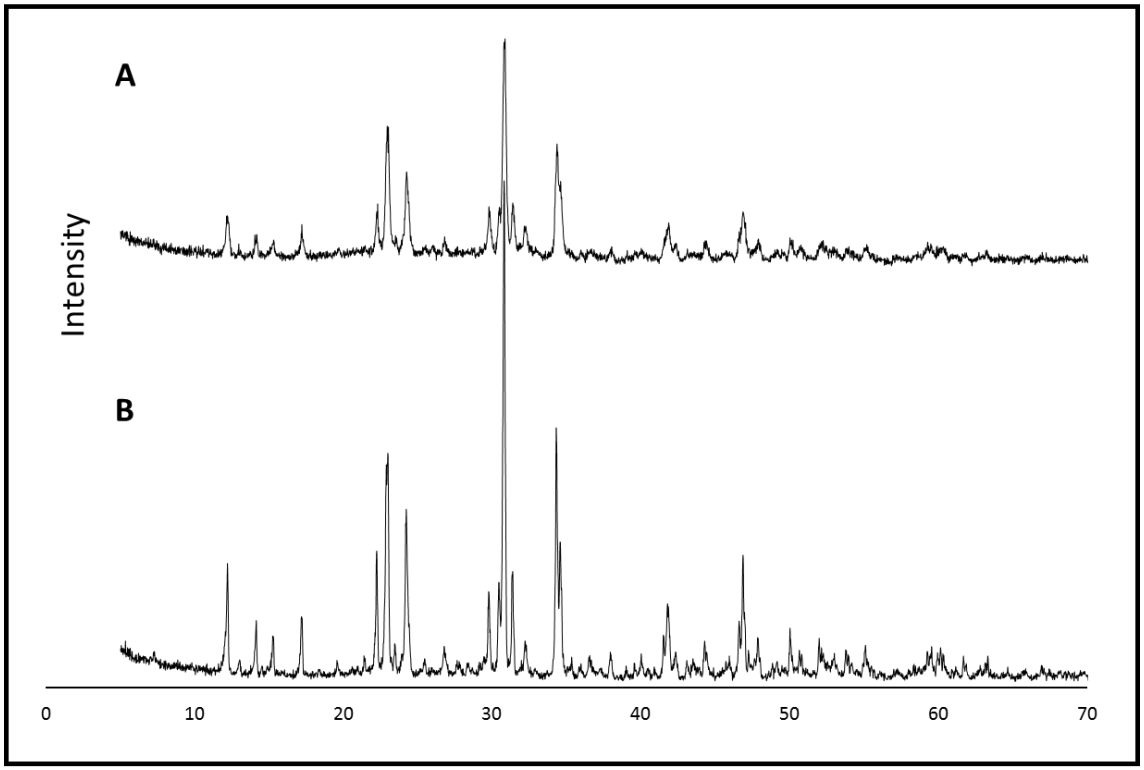


Fig. 4.

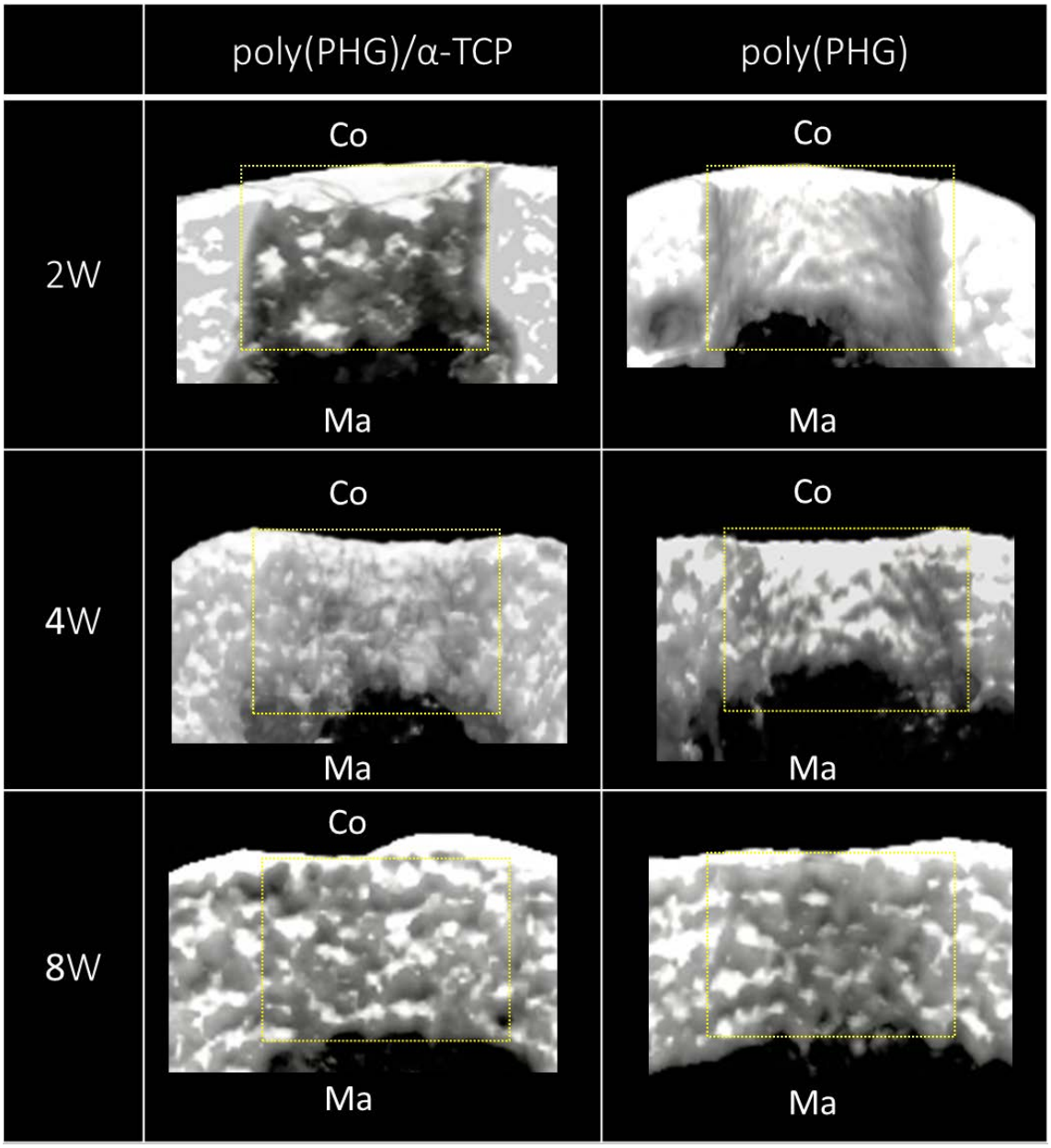


Fig. 5.

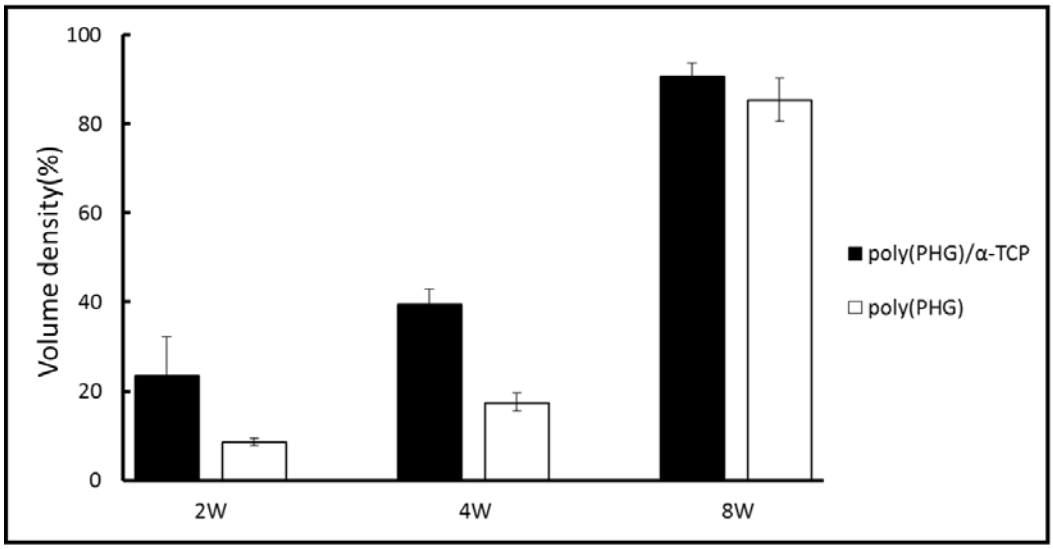


Fig. 6.

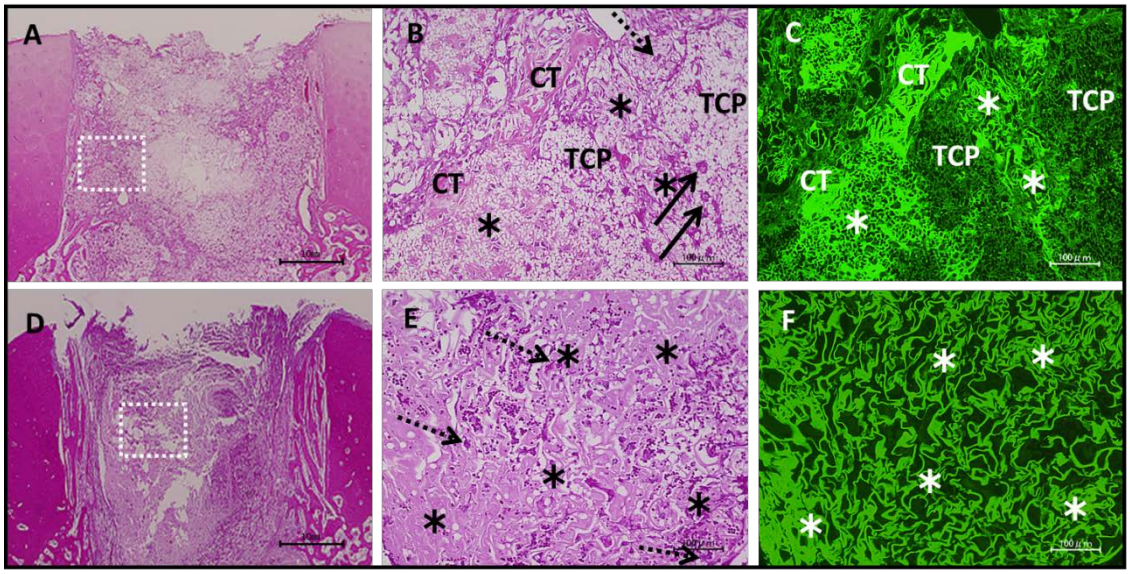
A
B
CT
TCP
TCP
CT
C
CT
TCP
TCP
CT
D
E
F

Fig. 7.

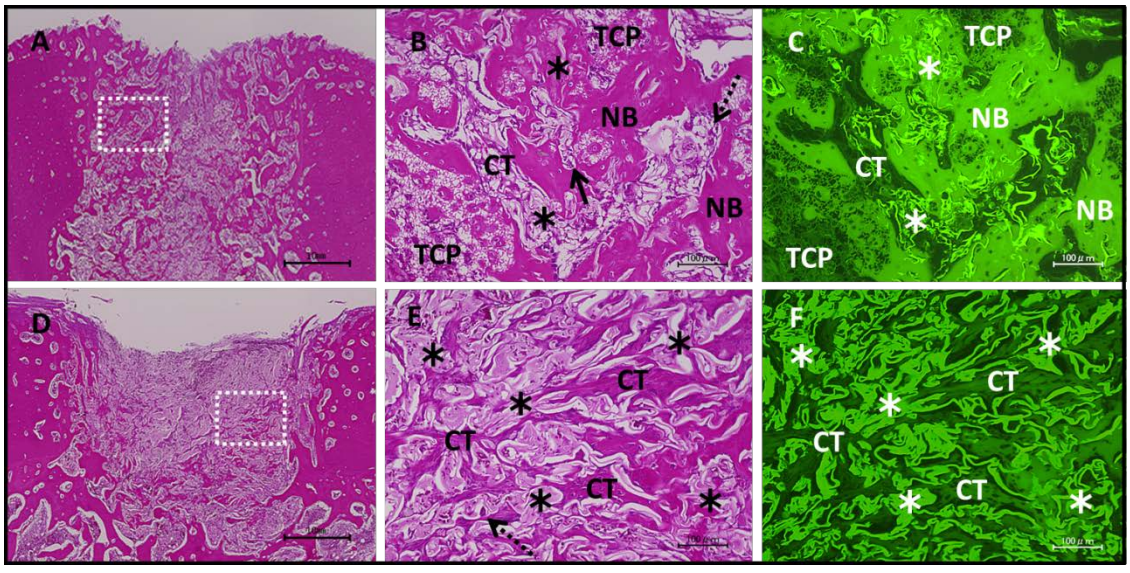
A
B
TCP
NB
CT
NB
TCP
C
TCP
NB
CT
NB
TCP
D
E
CT
CT
CT
F
CT
CT
CT

Fig. 8.

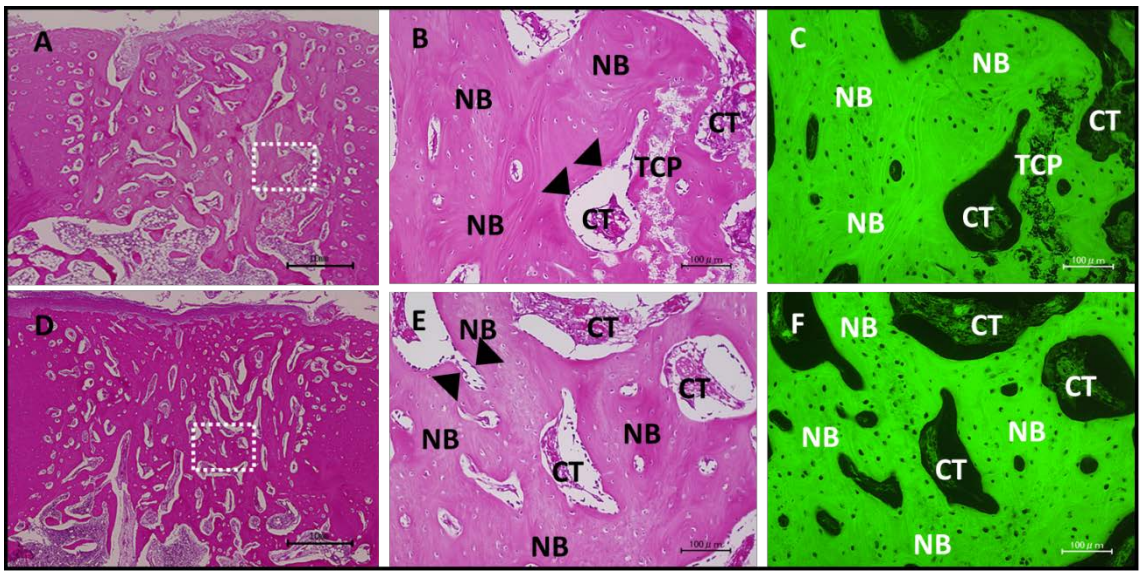
A
B
NB
NB
CT
TCP
NB
CT
C
NB
NB
CT
TCP
NB
CT
D
E
NB
CT
CT
NB
NB
CT
NB
F
NB
CT
CT
NB
NB
CT
NB

Fig. 9.